Theor Chem Account (2007) 118:549–556
DOI 10.1007/s00214-007-0344-0

REGULAR ARTICLE

# Externally steered relaxation of tight polyethylene tangles with different initial knot topologies

**Gustavo A. Arteca**

Received: 5 January 2007 / Accepted: 5 March 2007 / Published online: 7 June 2007


**Abstract** Using single-molecule manipulations or sudden changes in solvent, it is possible to introduce knotted-loops (or "tangles") in open linear polymers. It is still unclear how these tangles relax, and in particular, whether it is possible to trap knots locally by adopting very compact loop conformations. Here, we use steered molecular dynamics simulations to study a highly stressed polyethylene chain with three different knot topologies. Starting from stressed configurations, unknotting events are recognized as leading to sudden transitions in overcrossing number. By means of a soft compressing external force, we show that: (1) tangles with different complexities can be unknotted and (2) the potential energy decreases in a way that suggests that a similar relaxation mechanism might be at work for all the tested loop topologies.

**Keywords** Polymer knots · Polymer stretching · Steered molecular dynamics · Knot localization

## 1 Introduction

A mathematical knot is a closed loop with a *permanent* topological constraint due to self-entanglement; its unknotting is prevented by disallowing loop self-intersections. In open loops, the constraint becomes *transient*, though it may persist for a long time in a real chain. In this work, we consider transient entanglements in linear polymers, referred to as *one-dimensional* (1D) *tangles*, " *open knots*", or " *knotted-loops*" [1]. The formation of 1D tangles is *not* a rare event. In fact, the probability of self-knotting increases as $1-e^{-an}$, where $n$ is the number of monomers [2]. Open knots have been seen in isolated [3,4] and externally driven polymers [5,6], and also in macroscopic metalic chains [7,8]. Local knotting is also facilitated by diffusion within compact conformations, such as those adopted by a chain in a poor solvent [4] or when confined to small spaces [9,10].

Once a 1D tangle is formed, the locally knotted-loop may collapse to a very small size if the rest of chain swells in a good solvent [11]. Similarly, DNA can be tied into knots using optical tweezers; a sustained external tension produces highly localized 1D tangles [5,6]. It has been conjectured that rapid switches in solvent quality may be sufficient to trap a tight tangle within a long chain [11,12]. Yet, tight knots (e.g., in DNA chains) undergo thermal diffusion and can be remarkably mobile [5,7]. The dynamics of knot localization is also known to be a key factor to understand the change in gel electrophoretic velocities when DNA knots of various topological complexities are subject to weak and strong electric fields [13]. Under a strong field, simpler knots are more easily deformed and elongated, thereby migrating more easily in the polymer network of an agar gel [13].

For self-attracting ring homopolymers, knot delocalization is expected in the globular regime, while a weak knot localization is expected at the $\theta$-transition [14]. Results from shaken hanging chains also show that tight knots can form and disappear spontaneously, sliding and unknotting with an average time $\tau_U \sim n^2$ that is consistent with the diffusive behaviour of an $n$-bead chain [5,15]. Simulations also hint at distinct relaxation behaviours: whereas the equilibrium relaxation time of *closed loops* appears insensitive to the knot type $K$ [16], differences occur whenever the polymer is allowed to relax *after cutting* the knot [17]. It thus appears

Contribution to the Serafín Fraga Memorial Issue.

G. A. Arteca (✉)
Département de Chimie et Biochimie and Biomolecular Sciences Programme, Laurentian University,
Ramsey Lake Road, Sudbury, ON, Canada P3E 2C6
e-mail: gustavo@laurentienne.ca

that, by releasing the topological constraint, any excess free energy may be dissipated through nonequilibrium motions with time scales that depend on the loop topology, i.e., the original "knot type $K$" of the $K$-tangle [17]. Here, we consider a related problem, namely, the quasi-equilibrium relaxation of a *tight* tangle driven under conditions that simulate the external steering of an atomic-force microscope (AFM) tip or optical tweezers [18,19]. Two main issues are addressed: (a) the conditions under which a highly stressed knot could be trapped locally for a significant amount of time, and (b) whether this trapping is affected by the knot type in a one-dimensional $K$-tangle.

We study grafted polyethylene knotted-loops subject to periodic external perturbations. Given that this polymer has weak self-interactions, we expect knot relaxation to be mainly controlled by the energy flow induced by the mechanical force. Our approach applies the "soft" steered molecular dynamics (SSMD) algorithm [18,20,21] on tight loops in various topologies. In this simulation protocol, chains evolve under quasi-equilibrium conditions while applying periodic "pulls" or "pushes" on a single chain bond. This process allows for internal energy redistribution, while letting chains explore a range of rearrangements including those leading to knot swelling, diffusion, and unknotting. We show below that a weak compression elicits an unknotting transition common to many knots.

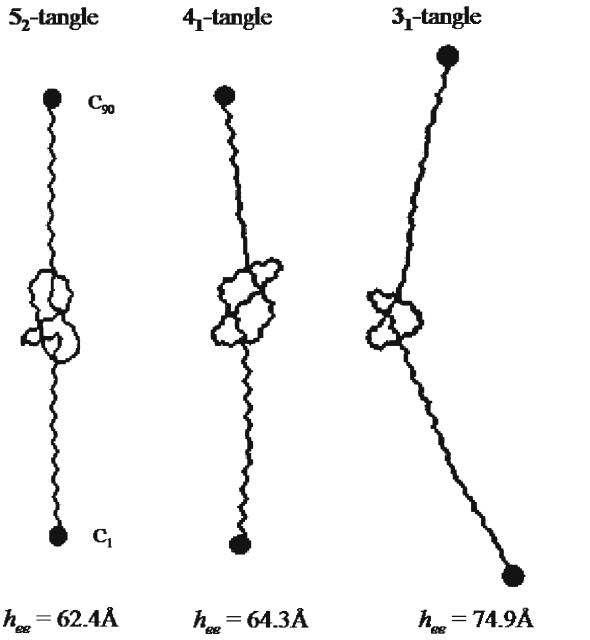


**Fig. 1** Starting configurations for the end-grafted $C_{90}H_{182}$ polyethylene $K$-tangles considered in this work (for clarity, hydrogen atoms are omitted). The tethers have a length consistent with a highly stressed central knotted-loop with a minimal mean size. The $h_{ee} = ||\mathbf{r}(C_1) - \mathbf{r}(C_{90})||$ end-to-end distances are given below. These conformers are subject to periodic compressing perturbations at the $C_{89} - C_{90}$ bond using the soft steered molecular dynamics (SSMD) protocol. Over time, stress is removed from all tangles and unknotting may take place with a probability that depends on the knot type

## 2 Protocols for steered compression dynamics and polymer shape analysis

We follow the compression of grafted $K$-tangles, found initially in very tight conformations. Three cases are compared: (a) the $3_1$-tangle (i.e., a "trefoil" knotted-loop), (b) the $4_1$-tangle (a "figure-8" twist knot), and (c) the $5_2$-tangle (also a twist knotted-loop). We have considered chains that, *whenever stress is absent*, adopt similar energies for all accessible topologies (including the unknot). For this reason, we use 90-carbon polyethylene chains, $C_{90}H_{182}$; this number of carbon atoms ensures stable (i.e., not self-unknotting) and nearly degenerate *unstressed* configurations for the three $K$-tangles. (Shorter chains would be too stressed and may unknot through phantom crossings [22,23] or bond breaking [24], depending on how forces are modelled.) The unstressed tangles were generated by the protocol in Ref. [21]. From these, we derive tight loops by inducing an externally driven stretching transition [21]. The initial conformers appear in Fig. 1; they have comparable end-to-end distances $h_{ee} = ||\mathbf{r}(C_1) - \mathbf{r}(C_{90})||$, yet quite different initial potential energies. In this work, we confine ourselves to these particular three topologies because they are the only one that can be produced on a $C_{90}$ chain; comparing more complex knots would require longer chains.

### 2.1 Unknotting transitions during compression

The choice of the five-crossing $5_2$-tangle is dictated by the fact it has *two* possible unknotting channels. The unknotting transition in a open chain with a knotted-tangle is of course not defined unambiguously and it is a matter of interesting debate in the literature [25,26]. In our case, we have considered to two possible definitions to characterize the onset of "unknotting" in the present tangles. The first approach (illustrated in Fig. 2) is simple and intuitive, and it can be applied to trajectories that begin from tightly knotted configurations. As shown in Fig. 2, we can partition the space using the plane perpendicular to the last bond vector, denoted by $\mathbf{v}_A = \mathbf{r}(C_{90}) - \mathbf{r}(C_{89})$. Using the starting configuration, we define the half-space containing the knotted loop to be "above" the latter plane. We can thus define an "unknotting event" whenever the nearest neighbour beads to $\mathbf{v}_A$ on the loop appear *under the plane* (cf. Fig. 2). Alternatively, we have used a sudden variation in a convenient entanglement descriptor as an indicator of an unknotting event (see below).

Using thus the definition illustrated in Fig. 2, the symmetry of a torus $5_1$-tangle will produce a $5_1 \rightarrow 3_1$ transition if either end of the loop is unknotted, that is, if we "switch" the handedness of the first and fifth crossings in an oriented

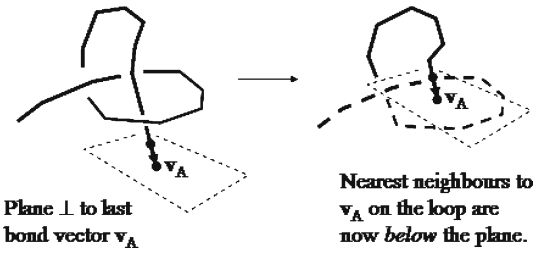


**Fig. 2** Schematic description of an "unknotting" event in an open chain polymer. As long as we are starting from a tight-knotted configuration (e.g., those in Fig. 1), the unknotting transition can be recognized by the change in relative location of the nearest neighbour polymer beads with respect to the plane perpendicular to the last bond vector $\mathbf{v}_A$. With this definition, the *left-hand side* scheme is "knotted," whereas the *right-hand side* configuration will be "unknotted"

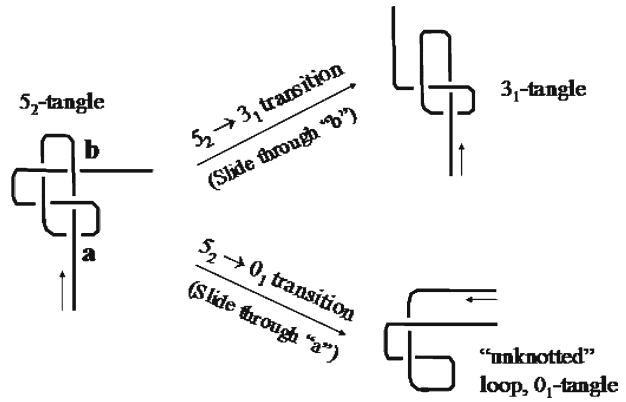


**Fig. 3** Different unknotting transitions in the $5_2$-tangle depending on which terminal bond crosses over a loop in an oriented chain. If the initial terminus crosses its nearest loop (crossing "a"), the $5_2$ decays directly to a $0_1$-tangle. In contrast, the last terminus produces a $3_1$-tangle if the crossing "b" is eliminated in the sense defined in Fig. 2. This $5_2 \rightarrow 3_1$ transition can then be followed by a second transition $3_1 \rightarrow 0_1$ in some cases. Note that a torus $5_1$-tangle would decay symmetrically to only $3_1$-tangles by undoing either terminal loop

chain. In contrast, the twist $5_2$-tangle is asymmetric and will produce two distinct "unknotting transitions", as explained in Fig. 3. Note thus that if the $C_1$-terminus is unknotted first (cf. Figs. 1 and 3), there will be an initial $5_2 \rightarrow 3_1$ transition. On the other hand, a $5_2 \rightarrow 0_1$ transition takes place when unknotting via the $C_{90}$-terminus. A $5_2$-loop "decayed" to a $3_1$-tangle (right-hand-side top diagram in Fig. 3) might in turn evolve into a $0_1$-tangle (or "unknot") by further relaxation. By choosing the $5_2$-tangle of $C_{90}H_{182}$, we can use the expected similar probability of the two unknotting channels as a control for the quality of the sampling during the MD simulations. Below, we discuss how these transitions can be recognized using a shape descriptor of polymer entanglement.

### 2.2 Steered molecular dynamics compressions

The initial conformers are in the stressed (or Pincus) regime [27,28], where the potential energy rises quadratically over the ground-state fluctuations. At maximum stress, the structures in Fig. 1 should include two long tethers and a collapsed region made of C* short hairpins, with C* the minimum number of crossings for the compact knotted-loop. Considering that a short hairpin requires ca. 10 carbon atoms [22,23], the tether length can be estimated as $n_{\text{tether}} \approx 1/2[n - 10\text{C}^*]$, where $n$ is the total number of atoms in the chain. For an $n = 90$ chain to form a strongly collapsed $5_2$-tangle (i.e., C* = 5), we would then expect two tethers with $n_{\text{tether}} \approx 20$. This estimate matches the structures in Fig. 1, and is therefore consistent with our claim that all the initial conformations in that figure are highly stressed (or "tight") $K$-tangles.

The algorithm for the SSMD compression differs from other MD approaches that apply a constant-force or constant-velocity pull (or push) at a point of the chain [27,28]. Our present protocol resembles the one used in Refs. [17–19], and can be summarized as follows:

(1) *First compressing step*: The $K$-tangles are modelled in the MM2 force field [29], with the $C_1$-atom permanently anchored. Initial atomic velocities are assigned from a Maxwell–Boltzmann distribution at $T_0 = 300\,\text{K}$; the temperature is kept constant with a simulated Berendsen thermal bath at $T_0$ [30]. To start an MD run, we introduce a slight compression on the initial conformation by shortening the last chain bond ($C_{89} - C_{90}$) to 1.3 Å, while re-accommodating the H-atoms bonded to $C_{90}$. After the compression, the $C_{90}$-atom is "anchored" (i.e., it is "frozen" with respect to molecular dynamics).

(2) *Relaxation step*: The compressed doubly anchored chain built in (1) is then allowed to evolve for $\Delta = 5\,\text{ps}$ coupled to the thermostat (using a relaxation constant of 100 fs and an integration step of 1 fs). During this period, the chain responds to the "soft" push by rearranging and redistributing the excess energy. Since the tangles start from a high-energy stretched conformation, the compression should, on average, *reduce* the potential energy. At high stress, the period $\Delta = 5\,\text{ps}$ is too short for full re-equilibration at 300 K. In contrast, at sufficiently low stress levels, $\Delta$ is sufficient to dissipate any sharp peak in potential energy introduced by the external compression of a single bond [18].

(3) *Periodic compression/relaxation steps*: After the $\Delta$ period, a new perturbation is introduced by shortening again the $C_{89} - C_{90}$ bond on the last conformer generated in (2). The local geometry for the rest of the chain, and all atomic velocities, are kept the same as those at $t = \Delta$ . This step ensures dynamic continuity while mimicking the effect of an external force acting on a single bond. Note that the direction of compression would have changed in general with respect to that in (1). After restoring the $C_{90}$ anchoring, the new chain

conformation is allowed to evolve for another $\Delta$ period; both $C_1$ and $C_{90}$ do not move, but they affect the dynamic behaviour of all atoms attached to them. The procedure continues as a sequence of compression/relaxation steps for a period sufficiently long so as to remove all stress and reach the equilibrium energy at 300 K.

For the three tight $K$-tangles, 1,000 ps-SSMD trajectories are sufficient to remove all stress. Conformational snapshots are selected every 1 ps along each MD run, including the compression steps. The average behaviour is estimated from an ensemble of 20 independent SSMD runs, each starting from a different random distribution of initial atomic velocities.

### 2.3 Descriptors of polymer self-entanglement

We monitor the $K$-tangle relaxations (including their possible unknotting) using polymer shape descriptors. In cases of external steering, mean size descriptors (e.g., the radius of gyration) may be inadequate as they do not distinguish among many configurational rearrangements [20]. Descriptors of chain entanglement derived from knot-theory provide a better tool [31–34].

Self-entanglement complexity can be expressed in terms of $\{A_N\}$, the probability distribution of *projected crossings* (or "overcrossings") of backbone bonds [31]. The mean overcrossing (or "average crossing") number $\bar{N}$ is the number of projected bond–bond crossings averaged over all three-dimensional rigid projections of a given conformation [31]. Formally, we can write:

$$\bar{N} = \sum_{N=0}^{\max N} N A_N = (4\pi)^{-1} \int_{S^2} N(\mathbf{r}) \mathrm{d}\mathbf{S}(\mathbf{r}), \qquad (1)$$

where $N(\mathbf{r})$ is the crossing number for a projection to a plane tangent to the unit sphere $S^2$ at $\mathbf{r}$, with a surface element $\mathrm{d}\mathbf{S}(\mathbf{r})$. In practice, we evaluate Eq. (1) using a large set of uniformly distributed random projections to planes tangent to the smallest sphere enclosing the $K$-tangle [18,20,21,31,33].

The $\bar{N}$ descriptor belongs to a class of quasi-topological invariants of knot-type complexity [32–34]. and it correlates with observables such as gel velocities or sedimentation rates of knotted DNA [28]. Previously, we have used this descriptor to study free polymer dynamics (e.g., protein folding–unfolding transitions) [33,35], as well as the stretching dynamics of grafted peptides [21] and polyethylene $3_1$-tangles [20]. Here, we monitor the time evolution of $\bar{N}_K(t)$ for the reverse process, i.e., the possible unknotting of a stretched $K$-tangle due to a *compressing* bias. For the conformers in Fig. 1, the initial values are: $\bar{N}_{3_1}(0) = 5.99 \pm 0.05$, $\bar{N}_{4_1}(0) = 8.61 \pm 0.09$, and $\bar{N}_{5_2}(0) = 10.09 \pm 0.07$. From these values, we can expect the following possible changes in $\bar{N}$:

(a) If a chain buckles under compression without relaxing the knot, the mean overcrossing number should remain nearly constant since projected crossings between long tethers contribute little to $\bar{N}$.
(b) If the $K$-tangle relaxes and swells under compression, we should expect a shortening of the tethers and therefore an increase in $\bar{N}$ values.
(c) A relaxation leading to unknotting will appear as a sharp decrease in $\bar{N}$; in particular, a $5_2 \rightarrow 0_1$ transition should produce the maximum change in descriptor values. The $5_2 \rightarrow 3_1$ decay mode would elicit a smaller transition in $\bar{N}$.

Indeed, we propose the notion that some of these changes in $\bar{N}$ should be sharp enough to provide *an operational criterion* to recognize an "unknotting transition." This idea is illustrated well in Fig. 4, which shows a typical example of a SSMD trajectory with clear transitions in $\bar{N}$ value. The sharp decrease in $\bar{N}$ (at the point indicated with an asterisk, $t \approx 725$ ps) is probably the best indicator of a $5_2 \rightarrow 3_1$ "unfolding event." Moreover, a second large oscillation observed at $t \approx 900$ ps matches the onset of a $3_1 \rightarrow 0_1$ transition (defined with the criterion in Fig. 2). In practice, as long as one begins from a tight-knotted loop, *we can assign reliably the first sharp drop in $\bar{N}$ value to an unknotting transition*.

In the next sections, we discuss the compression of tight tangles and describe their mechanism in terms of energy relaxation and variations in mean overcrossing number. In nearly all cases, the unknotting in tight $K$-tangles defined operationally by a sudden change in $\bar{N}$ coincides well with the definition based on the relative location of the last bond vector and its nearest neighbours on a loop (cf. Fig. 2).

## 3 Steered relaxation and unknotting of tight $K$-tangles

The initial structures in Fig. 1 span a large energy range. If $E_{\mathrm{pot}}^{(K)}(t)$ denotes the potential energy at 300 K and time $t$ for a chain initially found as a $K$-tangle, then we have: $E_{\mathrm{pot}}^{(5_2)}(0) = 721$ kcal/mol, $E_{\mathrm{pot}}^{(4_1)}(0) = 445$ kcal/mol, $E_{\mathrm{pot}}^{(3_1)}(0) = 371$ kcal/mol. We find that an external compression always produces a *relaxation*, i.e., a removal of stress leading to a systematic decrease in $E_{\mathrm{pot}}^{(K)}(t)$ over time.

Figure 5 overlaps the $E_{\mathrm{pot}}^{(K)}(t)$ curves for 20 SSMD trajectories of each $K$-tangle. All chains reach a common equilibrium energy $E_{\mathrm{eq}}^{(\mathrm{chains})}$ at $t = 1,000$ ps, estimated as $E_{\mathrm{eq}}^{(\mathrm{chains})} = 310 \pm 20$ kcal/mol and denoted by the right-hand side error bar. As control, we have computed the average potential energy $< E_{\mathrm{pot}} >$ at 300 K for an *unknotted* $C_{90}H_{182}$ chain at equilibrium, as well as for *unstressed* knotted-loops. Both cases give $< E_{\mathrm{pot}} >= 315 \pm 25$ kcal/mol, which agrees with $E_{\mathrm{eq}}^{(\mathrm{chains})}$. This result shows that stress is fully removed

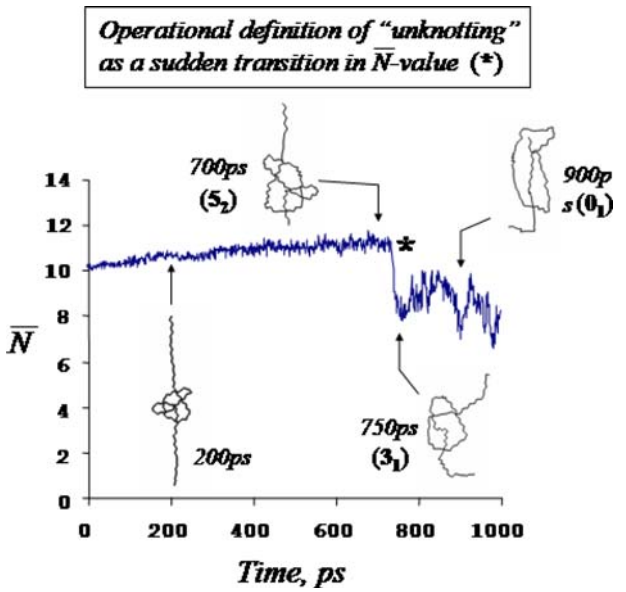


**Fig. 4** "Unknotting events" as sudden transitions in the mean overcrossing number $\bar{N}$. The diagram indicates a MD-trajectory for the steered compression of an initially tight grafted $5_2$-tangle (cf. Fig. 1). The central "knotted loop" is swollen up until $t \approx 700$ ps, leading to a small increase in $\bar{N}$. The sharp decrease in $\bar{N}$ at the point indicated by an asterisk ($t \approx 725$ ps) is taken, by definition, as an *unknotting event*; in this case, it corresponds to a $5_2 \rightarrow 3_1$ transition. Its further $3_1 \rightarrow 0_1$ transition is harder to recognize, but it coincides with another large oscillation in $\bar{N}$ at $t \approx 900$ ps

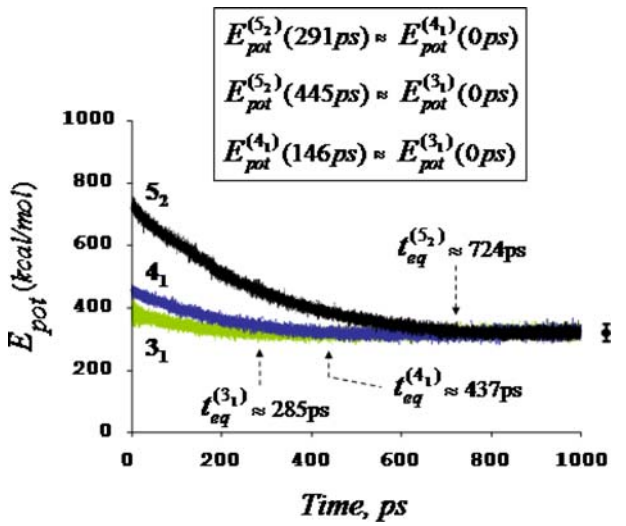


**Fig. 5** Decrease of potential energy $E_{\rm pot}(t)$ during the steered relaxation of polyethylene $K$-tangles. The *right-hand* side error bar corresponds to the energy fluctuations at equilibrium for the unknot and unstressed knots. The $t^{(K)}_{\rm eq}$-values correspond to the time where the $K$-tangle reaches equilibrium. The values on top show the $t^{(K,K')}$-values, corresponding to the time it takes a $K$-knot to reach the initial potential energy of a less entangled $K'$-knot. Using these values to shift the corresponding curves, it can easily be shown that $E_{\rm pot}(t)$ follows a single relaxation behaviour that is not dependent on the knot type (see text)

by the SSMD compressions. This also suggests that, regardless of the persistence of knotted-loops, *no chain remains as a tight knot when compressing polyethylene*.

The potential energy decay can be characterized by the time $t^{(K)}_{\rm eq}$ needed by the $K$-tangle to reach full equilibration in absence of stress, i.e., $E^{(K)}_{\rm pot}(t^{(K)}_{\rm eq}) = E^{(\rm chains)}_{\rm eq}$. These characteristic times are:

$$t^{(3_1)}_{\rm eq} = 285 \pm 4\,{\rm ps}; \quad t^{(4_1)}_{\rm eq} = 437 \pm 4\,{\rm ps};$$
$$t^{(5_2)}_{\rm eq} = 724 \pm 4\,{\rm ps}, \qquad (2)$$

where error bars correspond to the $\pm 20$ kcal/mol fluctuation in the $E^{(\rm chains)}_{\rm eq}$ value at 300 K. These values provide a benchmark to determine the time required for the onset of unknotting.

The relaxation behaviour in Fig. 5 masks a number of different conformational responses. In all cases, we have observed that: (1) the $K$-tangles can persist in "knotted" form once the stress is removed, and (2) unknotting transitions do take place for all knot types. However, the probability of these events depends on the initial loop topology.

Figure 6 superimposes the evolution in entanglement complexity $\bar{N}$ for the SSMD trajectories that *conserve the initial knot type*. To the right, we indicate the fraction that these trajectories represent within the total ensemble. The conservation of loop topology can be recognized in the fact that there are no sudden drops in $\bar{N}$ values while compressing the initial tight knot. A behaviour common to all knot types emerges: the periodic compression removes the initial stress by swelling the knots, thereby shortening the two tethers and increasing the mean overcrossing number. A swelling of the central loop occurs in all $K$-tangles. This increase

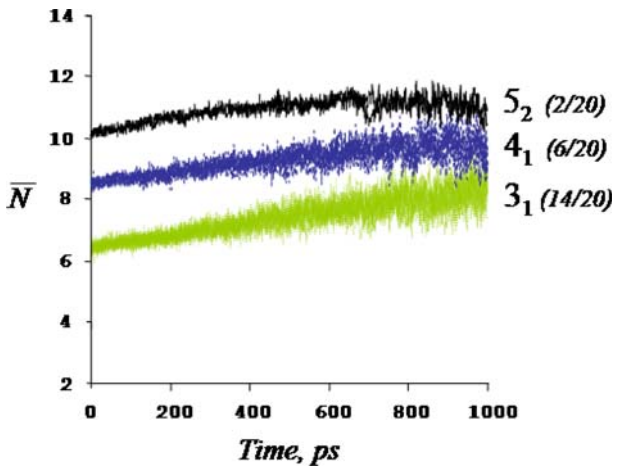


**Fig. 6** Evolution of the entanglement complexity $\bar{N}$ for SSMD trajectories where the central loops *remain knotted*. The *right-hand side* gives the unknotting frequency over 20 MD runs. Note that the more entangled loops unknot more often. This behaviour results from having chains of equal length, i.e., tethers whose lengths increase from the $5_2$- to the $3_1$-tangle

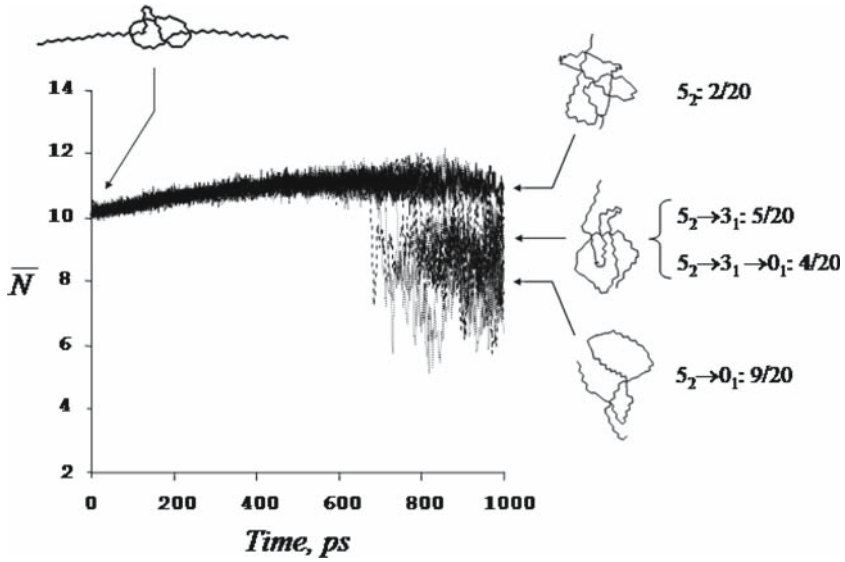


**Fig. 7** Mean overcrossing number $\bar{N}$ for 20 SSMD runs for the $5_2$-tangle. The pattern shows that this knotted-loop has approximately the same probability of sliding through the $C_1$ or $C_{90}$ termini. The $C_1$-sliding causes a $5_2 \rightarrow 3_1$ transition in 9 out of 20 trajectories; among these, 4 trajectories simplify further by undergoing a $3_1 \rightarrow 0_1$ transition. Similarly, the $C_{90}$-sliding causes a direct $5_2 \rightarrow 0_1$ transition also in 9 out of 20 trajectories. As denoted in Fig. 6, two trajectories conserve the initial $5_2$-tangle. The results indicate that the $3_1$-tangles generated by the $5_2 \rightarrow 3_1$ transition share the same shape features as *intact* (unstressed) $3_1$-tangles at 1,000 ps

in $\bar{N}_K(t)$ follows a similar pattern in all cases, although it is slightly faster for $3_1$-knots because the latter remove the initial stress more rapidly. At the end of the trajectories, all $K$-tangles are equally relaxed, and their differences in entanglement complexity are those that characterize the equilibrium values for the knotted-loops used as control at 300 K, i.e., $\bar{N}_{3_1} \approx 8.1$, $\bar{N}_{4_1} \approx 9.5$, $\bar{N}_{5_2} \approx 11.0$ at 1,000 ps.

In addition, we have observed evidence of knot mobility after relaxation, with a varying degree of displacement of the central loop either up or down the chain. However, our trajectory ensemble is too limited to: (1) ascertain any distinct trends in these motions that may depend on knot type and (2) the temporal dependence law for the loop diffusion.

Given that the present chains have the same contour length, their distinct unknotting probabilities correlate with differences in the length of the initial tethers. Having shorter tethers, the $5_2$-tangle appears to unknot more easily and soon after reaching the unstressed equilibrium configurations.

Figure 7 shows the pattern of unknotting transitions for the $5_2$-tangle. After 600 ps, there are drops in the entanglement descriptor; after the transitions, the $\bar{N}$ values have large fluctuations centred about $\bar{N} \approx 8$, consistent with the formation of grafted chains with the entanglement complexity of a relaxed $3_1$-tangle. Even though our trajectory ensemble is small, the observed distribution of "unknotting events" agrees well with the notion that the initial $5_2$-tangle should have a similar probability of unknotting into a $0_1$- or a $3_1$-tangle. Among the 18 trajectories leading to unknotting, we find nine transitions to the unknot ($5_2 \rightarrow 0_1$) and nine trajectories leading to a trefoil ($5_2 \rightarrow 3_1$). In turn, we find that the latter $3_1$-tangles have nearly equal probabilities to either remain as such or to unknot further through a $3_1 \rightarrow 0_1$ transition (5/20 and 4/20, respectively). This qualitatively correct pattern of relaxation and unknotting suggests that, despite the small sample size, the SSMD simulations can produce a reasonable survey of the configurational space accessible to $K$-tangles.

We can now estimate the differences in unknotting times. From the results in Fig. 7, we have computed the mean time $t_U$ for the first unknotting transition. An analysis for all $K$-tangles gives: $t_U(3_1) = 734 \pm 34$ ps (6 events), $t_U(4_1) = 814 \pm 122$ ps (14 events), and $t_U(5_2) = 819 \pm 91$ ps (18 events). These results do not yet represent the mean times for unknotting at equilibrium (i.e., $\tau_U(K)$) because different tangles start from slightly different levels of stress. We correct for these differences using the $t_{\mathrm{eq}}^{(K)}$ re-equilibration times, thereby estimating the unknotting times as $\tau_U(K) \approx t_U(K) - t_{\mathrm{eq}}^{(K)}$ :

$$\tau_U(3_1) = 449 \pm 38\,\mathrm{ps}, \quad \tau_U(4_1) = 337 \pm 126\,\mathrm{ps},$$
$$\tau_U(5_2) = 95 \pm 95\,\mathrm{ps}. \tag{3}$$

From Eq. (3), the $5_2$-tangle appears to unknot in near synchrony with the removal of stress. These results complement previous work in the literature which found that unknotting times increase with the number of essential crossings for knots *with the same knot size* [17]. In our case, chains have the *same contour length* and not the same knot size; the knotted-loop sizes are determined by the level of stress

conferred by the mechanical force. Under these conditions, a more complex tangle can unknot *faster* once the external stress has been fully removed, because it exhibits shorter tethers at equilibrium.

## 4 Relaxation dynamics in the potential energy

Despite differences in stability and unknotting times, the results in Figs. 5,6 and 7 show that an external steering leads to a controlled removal of stress in these three polyethylene tangles. The mechanism appears to involve the swelling of the knotted-loop, a shortening of the tethers and the equilibration at an energy level indistinguishable from that of the unknot. As shown below, the results in Fig. 5 also hint more quantitatively at a relaxation behaviour that may depend little on the knot type, at least in the case of the simplest topologies.

Based on these results, we conjecture that there seems to be a *unique* energy relaxation function, i.e., one law for the decay in the potential energy $E_{\rm pot}(t)$ over time for at least this class of short polyethylene $K$-tangles. We can check the validity of this hypothesis because it implies that the $E_{\rm pot}(t)$-functions for these $K$-tangles could be superimposed by shifting the time scale. To this end, we introduce $t^{(K,K')}$, corresponding to the time it takes a $K$-tangle to reach the initial potential energy of a $K'$-tangle, i.e., $E_{\rm pot}^{(K)}(t^{(K,K')}) = E_{\rm pot}^{(K')}(0)$, with $K'$ being a less entangled knot than $K$. The relevant values are (cf. Fig. 5):

$$t^{(5_2,4_1)} = 291 \pm 4\,\text{ps}, \quad t^{(5_2,3_1)} = 445 \pm 4\,\text{ps},$$
$$t^{(4_1,3_1)} = 146 \pm 4\,\text{ps}. \tag{4}$$

If the relaxation were to follow a single law, then $t^{(K,K')}$ would provide the shift in time scale needed to derive the potential energy of a $K$-knot from that of a less entangled $K'$-knot at time $t$:

$$E_{\rm pot}^{(K)}(t^{(K,K')} + t) = E_{\rm pot}^{(K')}(t), \quad \text{for all } t \geq 0. \tag{5}$$

We can now consider the corresponding re-equilibration times $t_{\rm eq}^{(K)}$ and $t_{\rm eq}^{(K')}$, defined in Sect. 3 as $E_{\rm pot}^{(K)}(t \geq t_{\rm eq}^{(K)}) = E_{\rm pot}^{(K')}(t \geq t_{\rm eq}^{(K')}) \approx E_{\rm eq}^{(\rm chains)}$. From this and Eq. (5), we expect the relation:

$$t^{(K,K')} + t_{\rm eq}^{(K')} = t_{\rm eq}^{(K)}. \tag{6}$$

This equality can be tested using the $\{t^{(K,K')}, t_{\rm eq}^{(K)}\}$ values evaluated before. Using Eqs.(2) and (4), we obtain: $t^{(5_2,4_1)} + t_{\rm eq}^{(4_1)} = 728 \pm 8\,\text{ps}$, which matches well the independent estimate $t_{\rm eq}^{(5_2)} = 724 \pm 4\,\text{ps}$. Similarly, the relation between the $5_2$- and $3_1$-tangles gives: $t^{(5_2,3_1)} + t_{\rm eq}^{(3_1)} = 730 \pm 8\,\text{ps}$, which again agrees with $t_{\rm eq}^{(5_2)}$. For the $4_1$- and $3_1$-tangles we get: $t^{(4_1,3_1)} + t_{\rm eq}^{(3_1)} = 431 \pm 8\,\text{ps}$, also in agreement with $t_{\rm eq}^{(4_1)} = 437 \pm 4\,\text{ps}$. Finally, we have verified that a shift by the corresponding $t^{(K,K')}$-values allows us to superimpose qualitatively the three entire potential energy curves in Fig. 5.

While Eq. (6) appears to be valid for tight $K$-tangles, other relations supported by our results are probably not general. For example, we have: $t_{\rm eq}^{(4_1)} + t_{\rm eq}^{(3_1)} = 722 \pm 8\,\text{ps}$, which also matches the $t_{\rm eq}^{(5_2)}$-estimate. According to Eq. (6), we would only expect: $t_{\rm eq}^{(4_1)} + t_{\rm eq}^{(3_1)} = t_{\rm eq}^{(5_2)} + \{t_{\rm eq}^{(4_1)} - t^{(4_1,3_1)} - t^{(5_2,4_1)}\}$, but the last term cancels out fortuitously in the present simulations: $t_{\rm eq}^{(4_1)} - t^{(4_1,3_1)} - t^{(5_2,4_1)} = 0 \pm 8\,\text{ps}$. As far as we know, there is no reason to believe that a relation such as $t_{\rm eq}^{(K')} \approx t^{(K,K')} + t^{(K',K'')}$ should not be valid for other triplets of knots.

## 5 Conclusions

Simulations based on simple square-well potentials indicate that knots and tangles can segregate their crossings into small tight regions as a result of applying a constant stretching force [36]. A similar collapse to tight knots is still observed as the dominant behaviour in more realistic potentials and stretching protocols [20]. Under conditions of weak and intermediate forces, the mean sizes of these knots follow the same scaling laws that apply to linear polymers [36]. In our case, we have considered the relaxation of some simple loops in the *tight knot regime* where these laws do not apply; here, the initial mean size is determined by the swollen nature of the portion of the chain that is not knotted.

Starting from three different tight knots in polyethylene, we have shown here that a controlled relaxation mediated by a external force *can undo* a collapsed knotted-loop, remove all excess potential energy stress, and eventually produce unknotting. Our results support the validity of Eq. (6) and suggest that a general law represented by Eq. (5) may be valid for at least of subclass of knotted-loops with different topologies. It remains to be seen whether a single simple mechanism for the relaxation of collapsed loop segments is observed in more complex knots. It could be possible that a new relaxation mechanism is present in composite knots. Exploring these interesting possibilities with a proper control set requires, however, a new series of knotted-loops built with longer polymers, because the present $C_{90}$-polyethylene chains can only sustain relaxed knotted-loops with up to five essential crossings. More complex topologies will unknot spontaneously in an unstressed $C_{90}$-chain.

Our results provide a benchmark to test the influence of other factors in the quasi-equilibrium relaxation of chains with topological defects. For instance, a different behaviour may occur when knotted-loops relax in the melt, as opposed to the present isolated chains. There is evidence that topological constraints in the melt change the self-diffusion

coefficient $D$ and the relaxation time $\tau$ in the autocorrelation function $C = \langle \mathbf{R}(t) \cdot \mathbf{R}(0) \rangle$, where $\mathbf{R}(t)$ is the span vector of a chain at time $t$ [37]. Whereas an isolated $n$-monomer chain with topological constraints behaves as a phantom chain in the melt (i.e., Rouse-like scaling with $D \sim n^{-1}$ and $\tau \sim n^2$), the presence of knots in the melt produces a different behaviour (with approximate scaling $D \sim n^{-1.59}$ and $\tau \sim n^{2.5}$) [37]. It is thus possible that inter-chain interactions may change the relaxation behaviour of tight tangles. Also, changes in composition (e.g., the introduction of stronger monomer–monomer interactions) may modify the relaxation mechanism and stabilize tight $K$-tangles. These issues will be addressed in future work.

**Acknowledgments** I thank Prof. Noham Weinberg (UCFV, Abbotsford, Canada) for a stimulating correspondence and Naomi Grant (Sudbury, Canada) for her comments on the manuscript. This research was supported by NSERC (Canada) and the Canada Research Chairs' Program. I dedicate this article to the memory of Prof. Fraga, teacher, mentor, and friend. I carry with me our talks on Science and Life, while looking at the Mediterranean in September, and the frosty trees of Alberta in January.

## References

1. O'Hara J (2003) Energy of knots and conformal geometry. World Scientific, Singapore
2. Sumners DW, Whittington SG (1988) J Phys A 21:1689
3. Wasserman SA, Cozzarelli NR (1986) Science 232:951
4. Brûlet A, Cotton JP, Lapp A, Jannink G (1996) J Phys II Fr 6:331
5. Arai Y, Yasuda R, Akashi K-I, Harada Y, Miyata H, Kinishita K, Itoh I (1999) Nature 399:446
6. Bao XR, Lee HJ, Quake SR (2003) Phys Rev Lett 91:265506
7. Ben-Naim E, Daya ZA, Vorobieff P, Ecke RE (2001) Phys Rev Lett 86:1414
8. Belmonte A, Shelley MJ, Eldakar ST, Wiggins CH (2001) Phys Rev Lett 87:114301
9. Arsuaga J, Vázquez M, Trigeros S, Sumners DW, Roca J (2002) Proc Natl Acad Sci USA 99:5373
10. Arsuaga J, Vázquez M, McGuirk P, Trigeros S, Sumners DW, Roca J (2005) Proc Natl Acad Sci USA 102:9165
11. Grosberg AY, Feigel A, Rabin Y (1996) Phys Rev 54:6618
12. Lai P-Y (1996) Phys Rev E 53:3819
13. Weber C, Stasiak A, DeLos Ríos P, Dietler G (2006) Biophys J 90:3100
14. Orlandini E, Stella AL, Vanderzande C (2003) Phys Rev 68: 031804
15. Belmonte A (2005) Knot dynamics in a driven hanging chain: experimental results. In: Calvo JA, Millett KC, Rawdon EJ, Stasiak A (eds) Physical and numerical methods in knot theory, including applications to the life sciences, series knots and everything, vol 36. World Scientific, River Edge, pp 65–74
16. Lai P-Y (2002) Phys Rev E 66:021805
17. Lai P-Y, Sheng Y-J, Tsao H-K (2001) Phys Rev Lett 87:175503
18. Arteca GA (2003) Phys Chem Chem Phys 5:407
19. Chtcheglova LA, Shubeita GT, Sekatskii SK, Dietler G (2004) Biophys J 86:1177
20. Arteca GA (2004) Phys Chem Chem Phys 6:3500
21. Arteca GA, Li Z (2004) Chem Phys Lett 399:496
22. Arteca GA (2000) Chem Phys Lett 328:45
23. Dhaliwal M, Weinberg N (2004) J Phys Org Chem 17:793
24. Saitta AM, Soper PD, Wasserman E, Klein ML (1999) Nature 399:46
25. Marcone B, Orlandini E, Stella AL, Zonta F (2005) J Phys A 38:L15
26. Shimamura MK, Kamata K, Yao S (2005) Phys Rev E 72:041804
27. Lu H, Isralewitz B, Krammer A, Vogel V, Schulten K (1998) Biophys J 75:662
28. Strick TR, Dessinges M-N, Charvin G, Dekker NH, Allemand J-F, Bensimon D, Croquette V (2003) Rep Prog Phys 66:1
29. Bukert U, Allinger NL (1982) Molecular mechanics. ACS Monographs, Washington DC
30. Berendsen HJC, Postma JPM, van Gunsteren WF, DiNola A, Haak JR (1984) J Chem Phys 81:3684
31. Arteca GA (1993) Biopolymers 33:1829
32. Stasiak A, Katritch V, Bednar J, Michoud D, Dubochet D (1996) Nature 384:122
33. Arteca GA, Reimann CT, Tapia O (2001) Mass Spectrom Revs 20:402
34. Shimamura MK, Deguchi T (2003) Phys Rev E 68:061108
35. Arteca GA, Tapia O (2004) Chem Phys Lett 383:462
36. Sheng Y-J, Lai P-Y, Tsao H-K (2000) Phys Rev E 61:2895
37. Brown S, Lenczycki T, Szamel G (2001) Phys Rev E 63:052801